

Article

# Heterogeneous Reservoir Petrophysical Property and Controlling Factors in Semi-Restricted Depositional Setting: A Case Study of Yamama Formation, X Oilfield, Middle East

Fengfeng Li \*, Lei Li, Haowei Chen, Wenyu Wang and Yang Wan

Research Institute of Petroleum Exploration and Development, Petrochina, Beijing 100083, China; lilei12@petrochina.com.cn (L.L.); chenhw02@petrochina.com.cn (H.C.); wangwy321@petrochina.com.cn (W.W.); ywan16@petrochina.com.cn (Y.W.)

\* Correspondence: lff1522188426@petrochina.com.cn

**Abstract:** The Early Cretaceous Yamama Formation of X oilfield, deposited in a semi-restricted setting, holds considerable oil reserves. However, the reservoir is extremely heterogeneous and is poorly studied. Integrating outcrops, cores, cast thin sections, regular or special core analysis, wireline logging data from six wells, and seismic data, this study provides an improved understanding of reservoir petrophysical characteristics and geological controlling factors including sedimentation, diagenesis, and sequence. The results showed that eight lithologies are developed in the Yamama Formation, of which packstone and wackstone are dominant. The physical properties span a wide range, with porosity mainly distributed between 10% and 25%, and the permeability mainly distributed between 0.1 mD and 1 mD. Nine types of pores are developed, with moldic pores, micropores, and skeletal pores being the most developed. The reservoir has six types of microstructures, of which the poorly sorted with mega-throat represent the best reservoir. The Yamama Formation was mainly deposited in a lagoon, along with five other facies, such as supratidal flat, patchy reef, back shoal, shoal, and open shelf. Six types of diageneses are developed, with dissolution during the penecontemporaneous stage being the most beneficial to the reservoir and cementation being the most destructive. Three sequences were recognized in the Yamama Formation. It concluded that the hydrodynamics in semi-restricted depositional setting is weak overall and does not have the potential to develop large-scale high-quality reservoirs. A wide range of bioclasts were selectively dissolved to form a large number of secondary pores. Sediments rich in *Algae*, *Bacinnella*, and peloids tend to form moldic pores, skeletal pores, and intergranular pores, respectively, which are prone to be favorable reservoirs. Controlled by the coupling of sedimentation and diagenesis driven by sequence, the reservoir is extremely heterogenous.

**Keywords:** Early Cretaceous; Yamama Formation; semi-restricted; bioclastic limestone; sedimentation; diagenesis; sequence



**Citation:** Li, F.; Li, L.; Chen, H.; Wang, W.; Wan, Y. Heterogeneous Reservoir Petrophysical Property and Controlling Factors in Semi-Restricted Depositional Setting: A Case Study of Yamama Formation, X Oilfield, Middle East. *J. Mar. Sci. Eng.* **2024**, *12*, 1011. <https://doi.org/10.3390/jmse12061011>

Academic Editors: Markes E. Johnson and Dejan Brkić

Received: 21 April 2024

Revised: 3 June 2024

Accepted: 13 June 2024

Published: 18 June 2024



**Copyright:** © 2024 by the authors. Licensee MDPI, Basel, Switzerland. This article is an open access article distributed under the terms and conditions of the Creative Commons Attribution (CC BY) license (<https://creativecommons.org/licenses/by/4.0/>).

## 1. Introduction

Yamama Formation of Late Berriasian to Early Aptian is one of the most important reservoirs in the Middle East [1]. Yamama Formation overlies the underlying Sulaiy Formation in a conformable manner and changes upward gradually into Ratawi Formation [2–5]. Yamama Formation will be used as a lithostratigraphic rather than a chronostratigraphic term because the formation may be dichronous [6]. During the late Berriasian–early Aptian period, many strata were deposited contemporaneously with the Yamama Formation but with different nomenclature, such as the well-known Habshan Formation in Oman, Minagish Formation in Kuwait, and the Fahliyan Formation in offshore Iran [7–11] (Figure 1). Yamama Formation is reported to contain hydrocarbons at 26 structures in southern Iraq [11], and it is also one of the most important oil-producing reservoirs [12].

To date, there are many studies on the Yamama Formation concerning petroleum generation [3,11,13,14], sedimentation [4,15–17], diagenesis [18,19], sequence [6], reservoir characterization [20,21], and geological modeling [22]. Many of them focus on one or a few oilfields, southeastern Iraq, or the Mesopotamian basin. Previous studies showed different views on reservoirs. Yamama Formation in Nasiriya oilfield, Southern Iraq, comprises outer shelf argillaceous limestone and oolitic, peloid, pelletal, and pseudo-oolitic shoal limestone [23]. Saleh (2014) proposed that red *Algae* and green *Algae* are concentrated in the upper and middle parts of the Yamama Formation in Ratawi field, respectively, and the non-skeleton grains included oolites, pellets, and micrite [15]. Oolitic packstone-grainstone facies were recognized in Yamama reservoir in West Qurna oilfield and the facies changed into a mixture of ooids, peloids with shell fragments, and algal debris in the lower part of the section [21]. Ahmed (2020) proposed that most of the porosity within Yamama Formation in the Faihaa oilfield was formed by diagenesis processes, implying that the Yamama reservoir is a type of diagenetic reservoir [18]. Different views on sequence have also been proposed, with the disagreement being divided into two or three sequences. Al Mafraji (2019) and Sadooni (1993) proposed that the Yamama Formation in southeastern Iraq [6,17] comprises three depositional cycles; however, Idan (2020) divided Yamama Formation into two main sequences in the Majnoon oilfield [4].

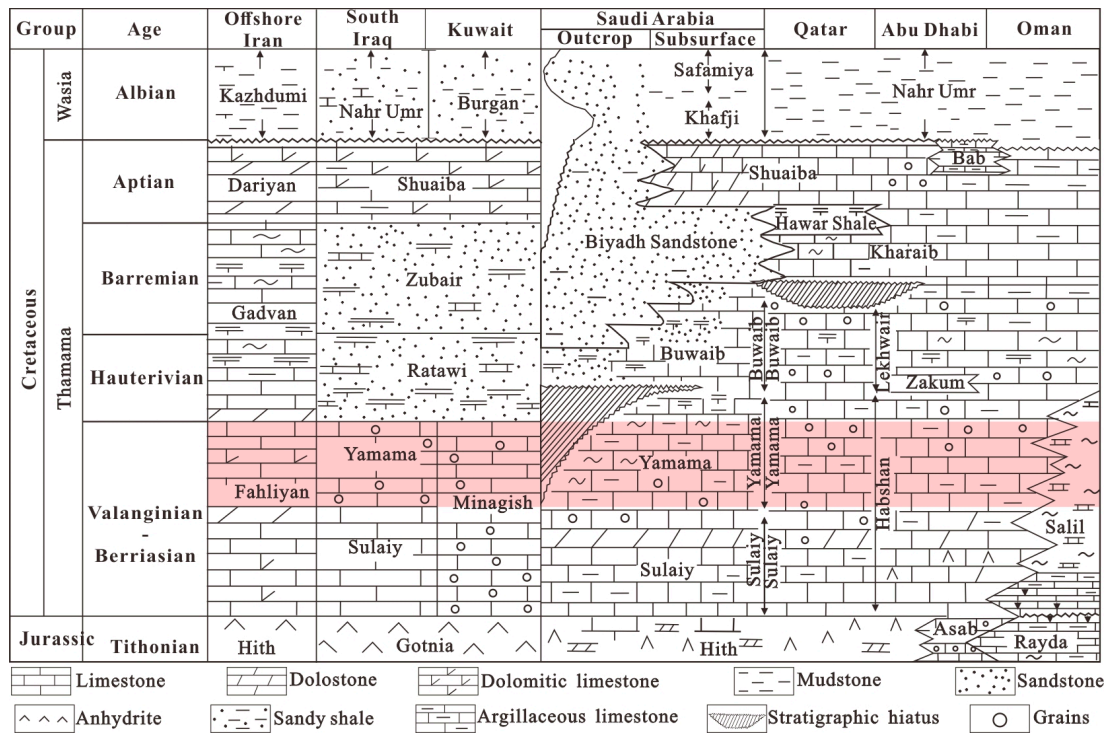


Figure 1. Chronostratigraphy of the Middle East, modified from [8–10].

X oilfield is located in the front zone of the Mesopotamian Basin. Compared with other oilfields, the X oilfield has a special paleogeographic location and reservoir property. The reservoir was formed in a semi-restricted depositional environment with low hydrodynamics and high clay content. Oolites are not developed in the sediments but instead in the diverse bioclasts. Therefore, the following questions are proposed. What are the petrophysical characteristics of the reservoir in a semi-restricted depositional setting? What is the potential for developing a favorable reservoir? What are the major geologic factors controlling reservoirs in semi-restricted depositional setting? Early studies with limited data reported that the Yamama formation in X oilfield developed into a thick homogeneous high-quality reservoir. With the abundance of data, it was found that the early understanding of the Yamama Formation needed to be updated. New data suggest that the reservoir

in Yamama Formation is more complicated than expected and that a low percentage of favorable reservoirs were developed. Furthermore, for Yamama Formation in X oilfield, the sedimentation, diagenesis, and sequence are less well studied.

The objectives of this work, therefore, taking the Yamama formation in X oilfield as an example, are to (1) investigate the reservoir lithology, physical property, and microstructure in a semi-restricted depositional setting; (2) establish a depositional model, diagenesis model, and sequence; and (3) unravel the reservoir heterogeneity and favorable reservoir potential in a semi-restricted depositional setting for production purpose.

## 2. Geological Setting

In mid-Tithonian times, evaporitic sedimentation in the Gotnia Basin abruptly ceased; deposition of very condensed deep shelfal and basinal organic-rich shales, marls, and micritic limestones occurred in the late Tithonian [24]. The relatively open Cretaceous basin, which succeeded the restricted Gotnia Basin, is best referred to as the “Balambo-Garau Basin” [25]. The opening of southern Neotethys permitted the exchange of open-marine waters between the Balambo-Garau and deep Neotethys Ocean [26]. By the early Cretaceous, southeastern Iraq is deposited in shallow marine conditions on a regionally extensive carbonate platform [18] (Figure 2).

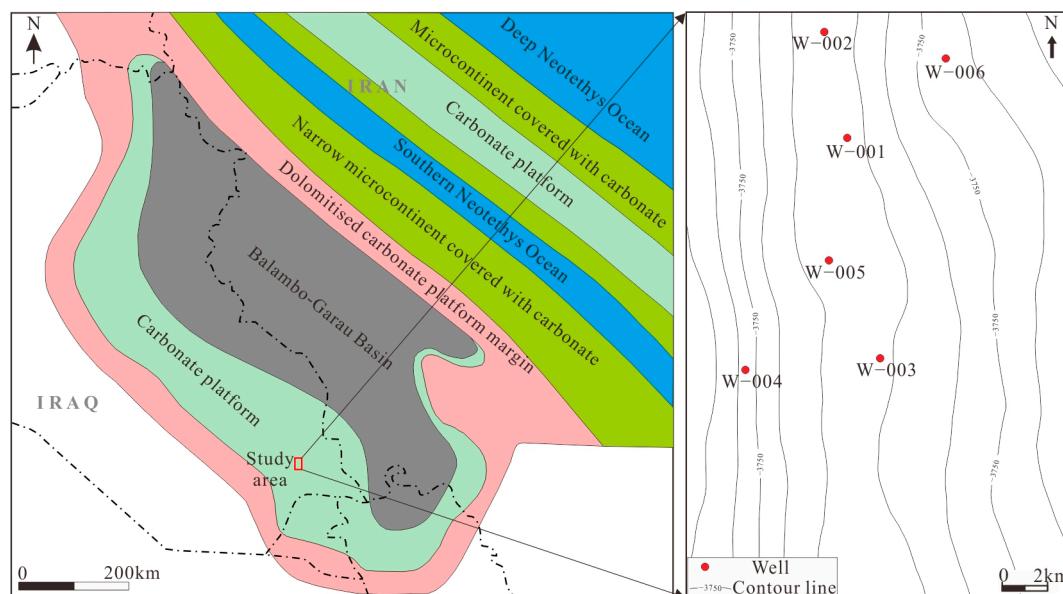


**Figure 2.** Early Cretaceous paleogeography map in the Iraq and Iran, modified from [26].

In the Berriasian to Valanginian periods, relatively continuous sedimentation took place in Oman, but most other parts of the Arabian Plate were affected by a late Valangian unconformity [27]. This interval is characterized by a moderately high, but falling, eustatic sea level [28]. The eastern shelf platform of the Arabian Plate was covered by shallow-water carbonates of the Yamama, Minagish, and Habshan formations, with the exception of the areas of the former Gotnia Province and the residual Arabian Basin, where argillaceous limestones of the Sulaiy/Makhul Formations were deposited [27]. The Yamama Formation in Iraq and the Habshan Formation in Oman both belong to the late Berriasian to early Valanginian period [6]. The upper part of the Habshan Formation consists of rudstone rich in coral and rudist fragments (Figure 3a). The middle part of the formation is grainstone dominated by oolites (Figure 3b). However, the Yamama Formation in southeastern Iraq is dominated by thick strata rich in *Algae*, peloids, *Bacinella*, and *Benthic foraminifera*. Oolites are never seen, and only a few coral fragment were seen in Yamama Formation in X oilfield. Both corals and oolites are indicative of an open, high-energy carbonate platform

margin, while *Algae*, peloids, *Bacinella*, and *Benthic foraminifera* are usually indicative of a semi-restricted, middle to low energy environment.

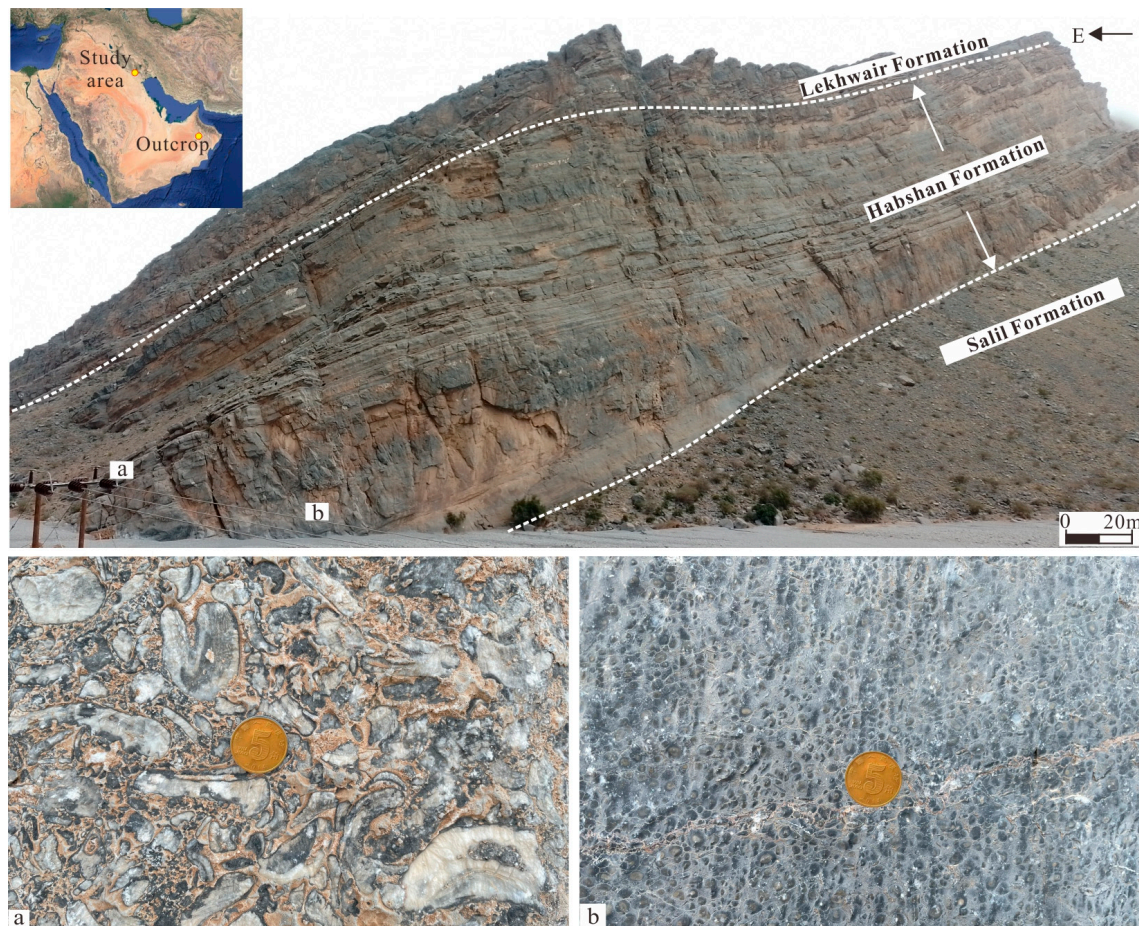


**Figure 3.** Outcrop of the Habshan Formation in Oman (equivalent of the Yamama Formation in southeastern Iraq). (a) Sampling in the middle of Habshan Formation, a large number of coarse rudist and coral fragment are visible; (b) Sampling in the lower of Habshan Formation, a large number of well sorted oolites are visible.

Therefore, during the late Berriasian to early Aptian period, the sedimentary hydrodynamics in southeastern Iraq was significantly lower than that in Oman. The Habshan Formation was deposited in a high-energy carbonate platform margin, while the Yamama Formation was deposited in a semi-restricted environment with weaker depositional hydrodynamics. The sedimentation of Yamama Formation is controlled by the Balambo-Garau Basin, as was the sedimentation of Minagish Formation in Kuwait, which is the equivalent of the Yamama Formation [7].

The average thickness of the Yamama Formation in X oilfield is about 300 m, and the depth ranges from 3500 m to 4200 m. The Yamama Formation is vertically divided into six lithological units, which, from top to bottom, are the Yamama Upper, the YRA, the YB-1, the YRB, the YB-2, and the YRC. YRA and YRB are important reservoir units. The YRC is heavily cemented or filled with bitumen and has poor physical properties. YB-1 and YB-2 serve as two permeability barriers [15], with YB-1 separating the YRA from the YRB. Due to the poor physical properties of YB-2 and YRC, they are not easily distinguished.

### 3. Materials and Methods

There are six wells drilled in the Yamama Formation in X Oilfield, of which five coring wells are among them (W-001, W-002, W-003, W-005, and W-006). The coring interval

covers all lithological units, with less coring in the Yamama Upper and no coring in the bottom of the YRC. In total, 685 m core, 881 cast thin section, 1547 physical properties, 140 mercury injection capillary pressure (MICP), and wireline logging from six wells, such as Gamma-ray (GR), bulk density (DEN), and resistivity (RT), are available in this study. In addition, more than 400 km<sup>2</sup> of 3D seismic data can be used.

The cores were described; lithology characterizations follow the classification schemes of Dunham [29], based on the depositional textures. Cast thin section samples were analyzed using a polarizing microscope; all were stained using Alizarin Red S to differentiate the dolomite from calcium carbonate. The pores type and pore volume could be identified by observation of cast thin section based on experience. The physical property was characterized by core plug analysis, wireline logging interpretation, and seismic inversion. Statistical bar charts, a permeability cross-section of six wells, and three porosity inversion plans are established and presented. The MICP data, which come from mercury intrusion experiments, are used to characterize microstructure, such as the pore throat size and sorting, and the microstructure was classified. Fourteen microfacies were identified in combination with five parameters such as indication biology, grain size, sorting, texture, and structure based on the sedimentation theory [30]. Five parameters were obtained from cast thin sections, of which indication biology and grain size were quantitatively counted, while the other parameters were qualitatively analyzed. Six depositional facies were classified according to the microfacies assemblage. Depositional facies interpretation was completed for all wells, and the contact relationships of all depositional facies were known according to Walther's law, and then a depositional model was finally established. The diagenesis type and effect on reservoir was investigated by cast thin sections and physical property data. Sequence stratigraphy framework relies on the identification of the key sequence boundary and maximum flooding surface (MFS). Finally, the distribution of favorable reservoir was clarified based on sedimentation, diagenesis, and sequence in combination with seismic inversion.

## 4. Result

### 4.1. Lithology

Based on the description of the 685 m core, the lithology of Yamama Formation in X Oilfield includes mudstone, wackstone, packstone, grainstone, rudstone, floatstone, and bindstone, of which the packstone and wackstone were the most developed. The lithology frequently changes vertically and is poorly correlated (Figure 4).

On Yamama upper member, only the W-001 well, W-002 well, and W-006 well were cored, and the cored interval consisted of thin dolomite, mudstone, packstone, and sparry grainstone, which is interbedded vertically.

The YRA is dominated by packstone and wackstone, followed by grainstone. The grainstone in W-006 well is intensely cemented. Thin mudstone can be seen in the W-005 well and thin rudstone can be seen in the W-003 well.

Thin interbedding of wackstone and dolomite in YB-1 and the W-001 well develops thick floatstone and thin cemented grainstone.

For YRB, the W-002 well and W-001 well are dominated by wackstone and packstone, with locally developed thick floatstone. Thin bindstone is developed at the bottom of the W-002 well. The W-006 well is dominated by thick wackstone, with locally thin packstone and grainstone. The W-005 well is dominated by thick wackstone with thin mudstone and packstone and locally developed dolomites. The core section is less in the W-003 well, consisting mainly of floatstone.

The coring interval is dominated by wackstone in the YB-2 member, in which the W-002 well developed thin grainstone.

The W-003 well and W-005 well were less cored in YRC and are dominated by wackstone with thin interbedded packstone and mudstone. The W-002 well is dominated by thick rudstone and wackstone. The W-006 well is dominated by thick wackstone and packstone with thin interbedded grainstone, both of which were intensely cemented.

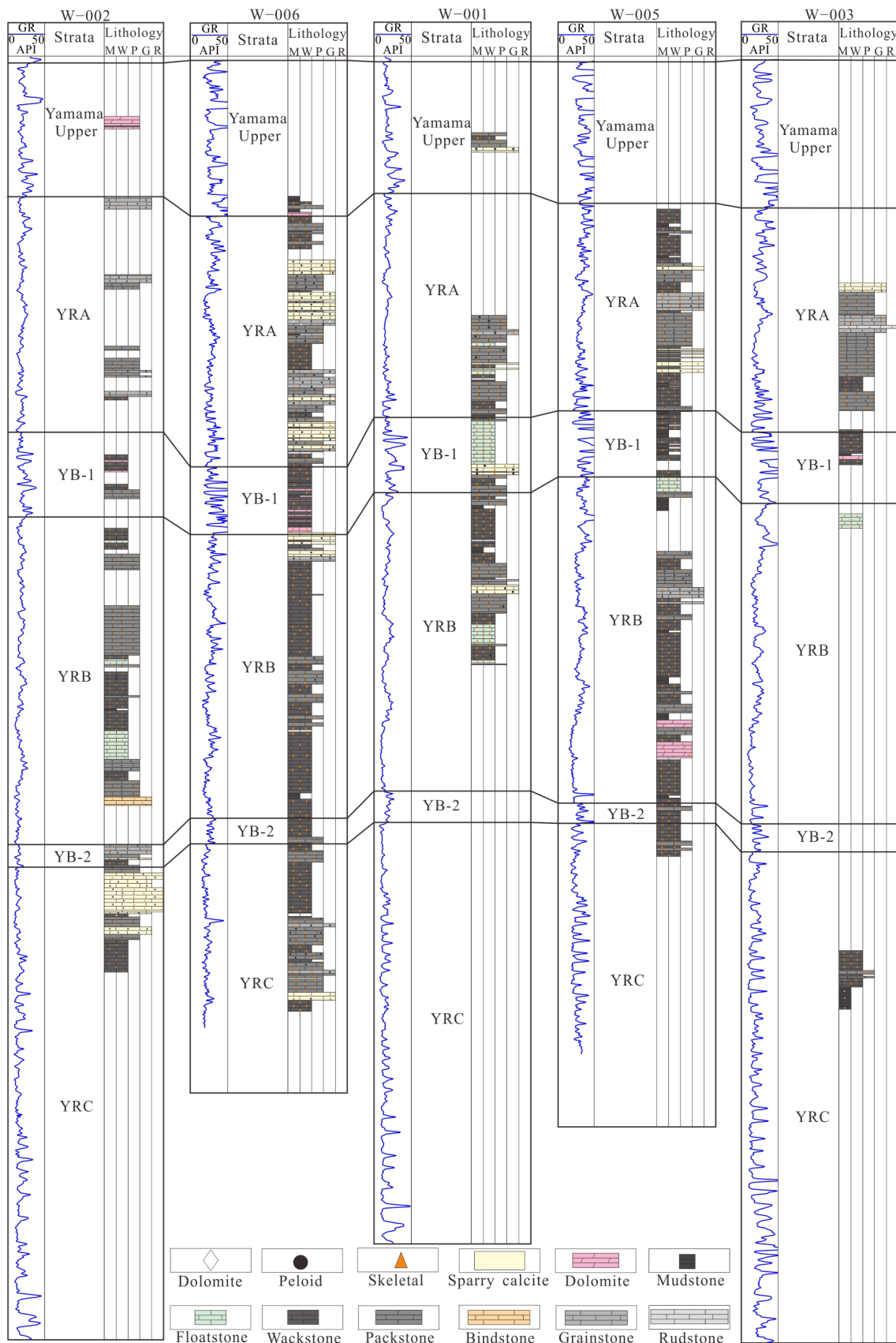
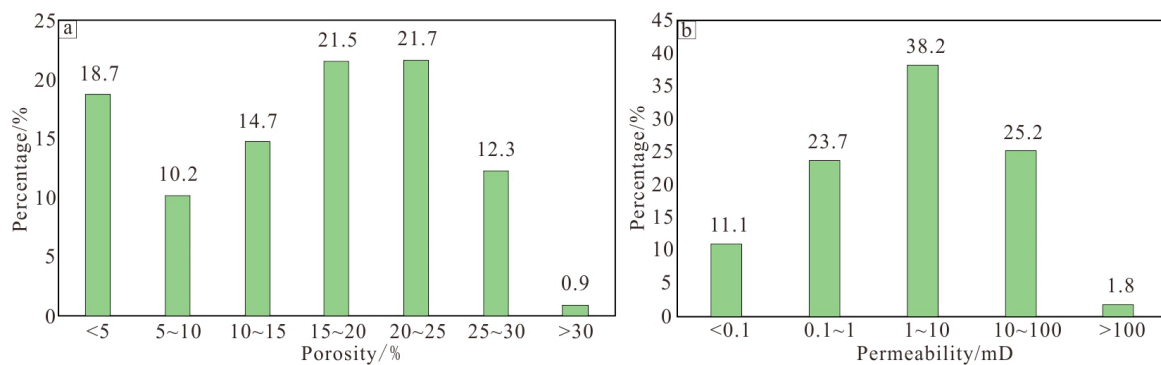


Figure 4. Lithology of cored interval in the X oilfield.

#### 4.2. Physical Property

Based on 1547 physical property samples, according to the evaluation criteria [31], the porosity is defined high porosity (>20%), medium porosity (10~20%), low porosity (5~10%), and poor porosity (<5%), and the permeability is defined high permeability (>100 mD), medium permeability (10~100 mD), low permeability (1~10 mD), extra-low permeability (0.1~1 mD), and tight (<0.1 mD). The results show that the physical properties of the Yamama Formation span a wide range. It is mainly medium porosity and high porosity, and the maximum can be greater than 30%, with a high proportion of low porosity and poor porosity (Figure 5a). The horizontal permeability differs by 1000 times, and the Yamama Formation is characterized by low permeability, followed by medium permeability and extra low permeability, and the proportion of high permeability is less developed (Figure 5b). It is important to note that these data only represent the physical properties of the coring interval.



**Figure 5.** Physical Properties of Yamama Formation in X oilfield (Data from core analysis). (a) Shows the distribution of porosity obtained from core analysis; (b) Shows the distribution of horizontal permeability obtained from core analysis.

Permeability from the wireline logging interpretation showed that the Yamama Formation, on the whole, has the highest proportion of tight reservoir, followed by extra-low permeability reservoir, and the proportion of low-, medium-, and high-permeability reservoirs is low. The permeability in each member varies greatly (Figure 6). The Yamama upper member is dominated by tight reservoirs, with small scale extra-low permeability reservoirs. The YRA member is dominated by extra-low permeability reservoirs, followed by low permeability reservoirs. The W-002 well develops a high proportion of medium permeability reservoirs, and two thin high permeability reservoirs are developed in the upper part of the well. The whole interval of YB-1 member is tight. The YRB member is dominated by extra-low permeability reservoirs, but low-, medium-, and high-permeability reservoirs are developed in relatively high proportions. The YB-2 member and YRC member are dominated by tight reservoirs. Small scale extra-low permeability reservoirs are locally developed.

Seismic inversion results show prominent lateral variations in porosity. Porosity inversion is not available for the W-002 well area because there are no seismic data. In the YRA member, porosity exhibits a trend of decreasing porosity from north to south, from middle to both flanks. The highest porosity is found in the W-001 and W-005 well areas (Figure 7a). The YRB member has the highest porosity, and it has a similar trend with YRA. The highest porosity is found in the W-005 well area (Figure 7b). The YRC member has an overall low porosity. The porosity of the two flanks is higher than that of the middle, and the highest porosity is found in the W-006 well area (Figure 7c).

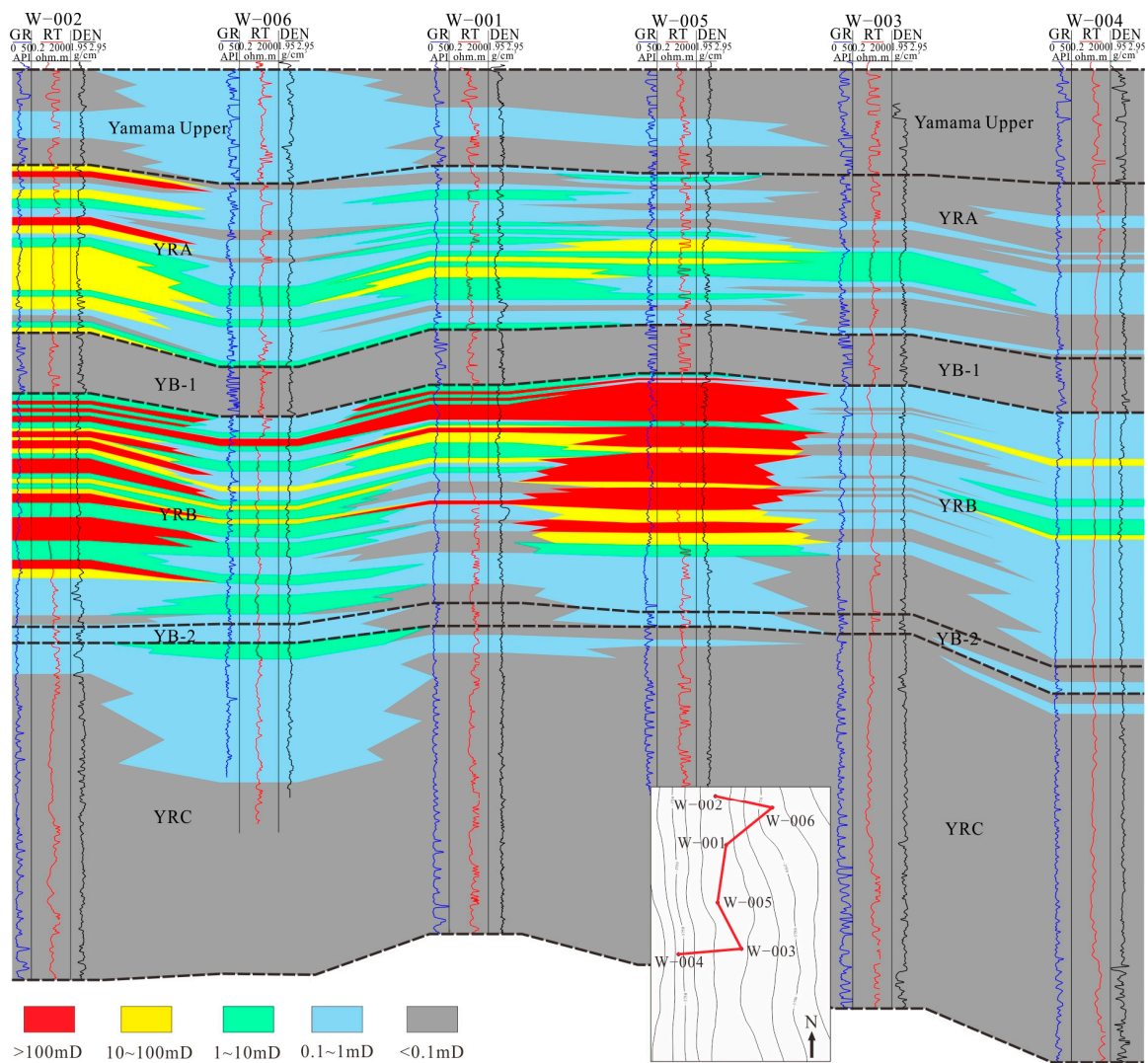


**Figure 6.** Permeability cross-section of the Yamama Formation (permeability from wireline logging interpretation).

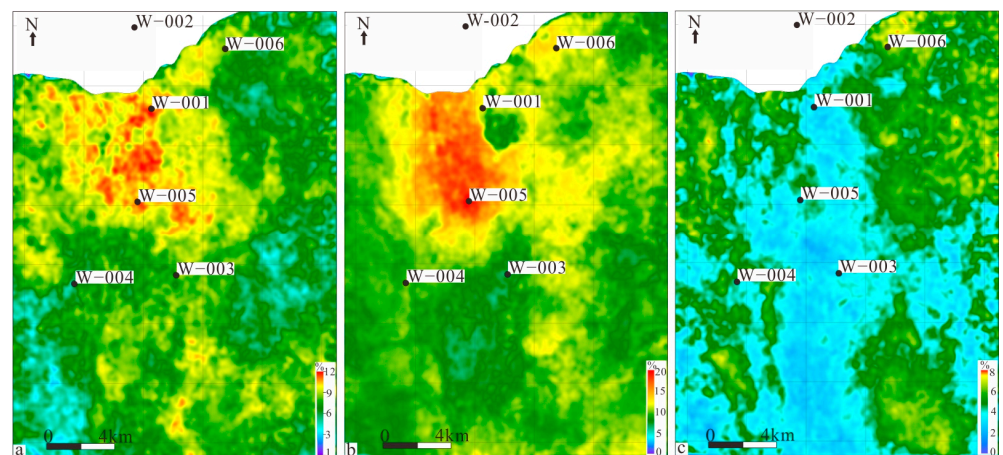


**Figure 7.** Porosity of the Yamama Formation in X oilfield (porosity from seismic inversion). (a) shows the distribution of porosity obtained from seismic inversion of YRA; (b) shows the distribution of porosity obtained from seismic inversion of YRB; (c) shows the distribution of porosity obtained from seismic inversion of YRC.

### 4.3. Pore Types

The 881 cast thin sections showed that the reservoirs of the Yamama Formation have diverse pores, including intergranular pores, intergranular dissolution pores, skeletal pores, vuggy pores, moldic pores, residual pores, micropores, intercrystal pores, and microfracture (Figure 8). Intergranular pores and intergranular dissolution pores are mainly developed in grainstone (Figure 8a–c), and the pores are uniformly distributed and well connected. Skeletal pores are mainly developed in wackstone or packstone (Figure 8d–f) and formed from *Benthic Foraminifera* or *Bacinella*. Skeletal pores in *Benthic foraminifera* are poorly connected and less developed (Figure 8d), whereas skeletal pores in *Bacinella* are usually developed in clusters, with larger pore volumes and better connectivity (Figure 8f). Vuggy pores and moldic pores are usually developed in wackstone and, to a lesser extent, in packstone (Figure 8g–i). Vuggy pores are usually larger than 2000  $\mu\text{m}$  (Figure 8g) and play an important role in porosity. Moldic pores, mainly formed by the dissolution of *Algae* and *Bivalves*, are usually isolated in micrite (Figure 8i). The size of the moldic pores is controlled by bioclastic, and fine bioclastic were dissolved to form small moldic pores (Figure 8j). Residual pores refer to the small amount of pore space remaining after the pores have been partially filled with cement, and the connectivity of the pores is usually poor (Figure 8k,l). Residual pores could develop in all kinds of lithologies. Micropores are mainly developed in micrite, which are difficult to see with the naked eye and are visible as hazy blue in stained cast thin sections (Figure 8m). Micropores have an important effect on porosity but have a small effect on permeability. Dissolution fractures are locally developed in the Yamama Formation (Figure 8n,o), connecting the isolated pores to each other, and have an important effect on permeability. Based on quantitative statistics, the Yamama Formation is dominated by moldic pores, skeletal pores, and micropores, followed by intergranular pores and vuggy pores, and the intergranular dissolution pores and intercrystal pores are less developed, with localized development of microfracture.

### 4.4. Microstructure

Based on 140 samples of MICP, the microstructure of the Yamama Formation was classified according to pore throat size and sorting. The pore throat is defined as either a mega-throat ( $>10\ \mu\text{m}$ ), macro-throat (2.5–10  $\mu\text{m}$ ), medium-throat (0.5–2.5  $\mu\text{m}$ ), micro-throat (0.075–0.5  $\mu\text{m}$ ), and nano-throat ( $<0.075\ \mu\text{m}$ ). The results show that the microstructure of the Yamama Formation can be divided into six types (I, II, III, IV, V, and VI). The Type I curves are multimodal, poorly sorted, with a relatively high proportion of mega- or macro-throats (Figure 9a). The Type II curves are unimodal with a broad peak, poorly sorted. They are dominated by medium throat, accompanied by a few macro-throats (Figure 9b). The Type III curves are unimodal with a relatively narrow peak and they are dominated by medium throats, relatively well sorted (Figure 9c). The Type IV curves are unimodal with narrow peaks. The throat radius is between 0.1  $\mu\text{m}$  and 1  $\mu\text{m}$  and well sorted. (Figure 9d). The Type V curves are bimodal. The primary peak is located at 0.5  $\mu\text{m}$ , and the secondary peak is roughly between 1 and 10  $\mu\text{m}$  (Figure 9e), which are poorly sorted. Type VI, whose pore-throat was less than 0.5  $\mu\text{m}$  overall, are mainly micro-throat and nano-throat, and are relatively well sorted (Figure 9f).

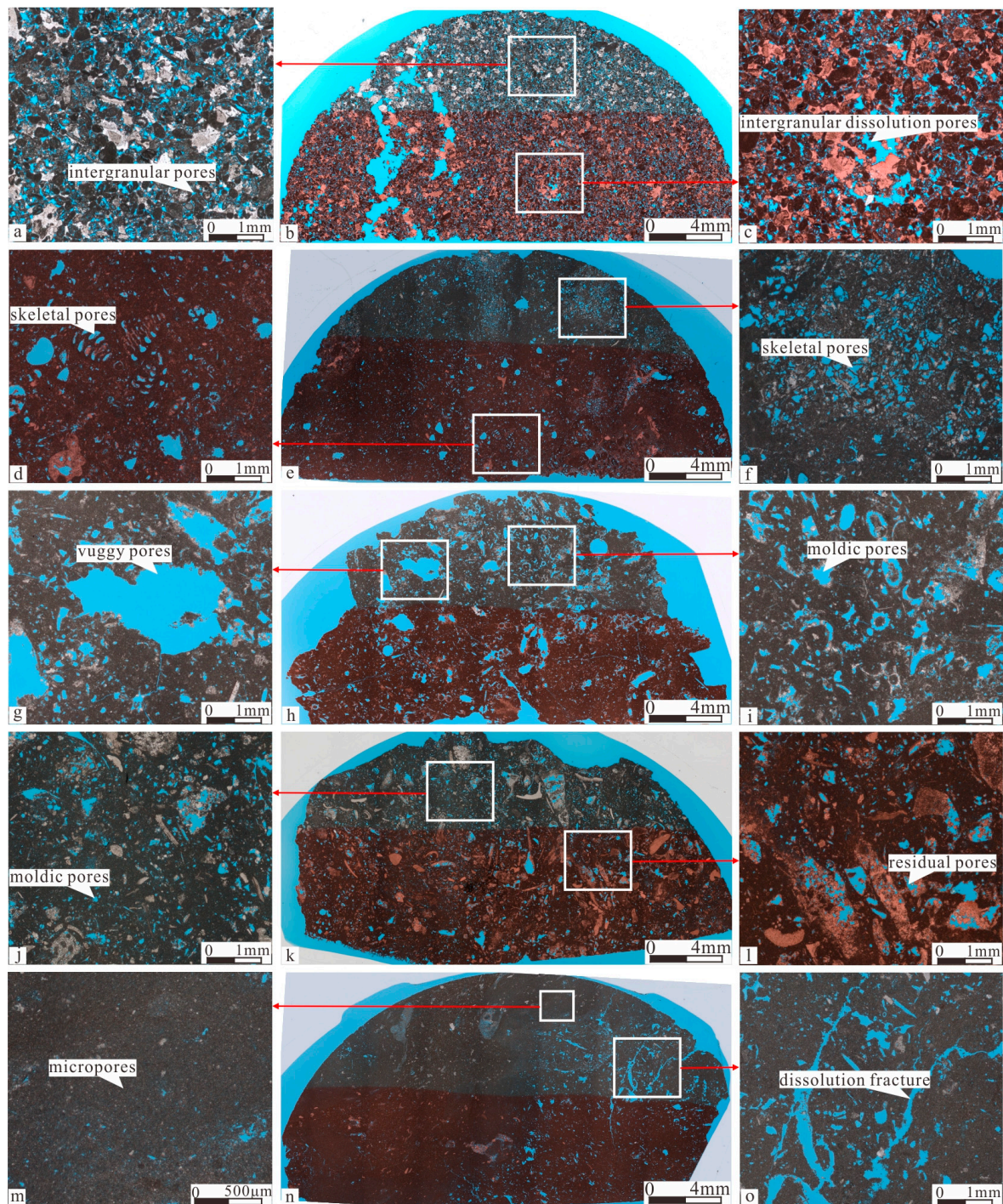


**Figure 8.** Pore types of Yamama Formation in X oilfield. (a) W-005 well, intergranular pores; (b) W-005 well, cast thin section panorama, grainstone; (c) W-005 well, intergranular dissolution pores; (d) W-005 well, skeletal pores formed from *Benthic Foraminifera*; (e) W-005 well, cast thin section panorama, wackstone; (f) W-005 well, skeletal pore formed from *Bacinella*; (g) W-005 well, vuggy pore; (h) W-005 well, cast thin section panorama, wackstone; (i) W-005 well, moldic pore formed from *Algae*; (j) W-005 well, moldic pore formed from fine bioclastic; (k) W-005 well, cast thin section panorama, packstone; (l) W-005 well, residual pores; (m) W-005 well, micropores; (n) W-005 well, cast thin section panorama, wackstone; (o) W-005 well, dissolution fractures.

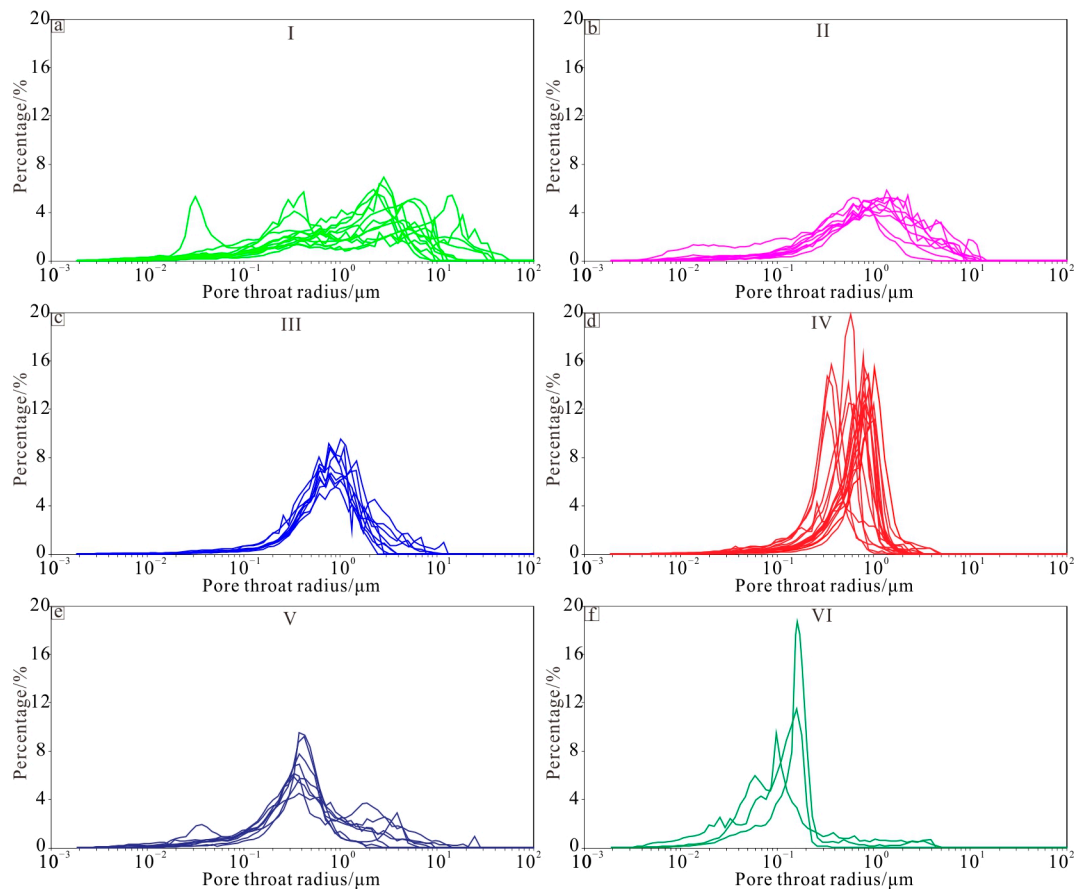


**Figure 9.** Microstructure of Yamama Formation in X oilfield. (a) The Type I, multimodal, poorly sorted; (b) The Type II, unimodal, poorly sorted; (c) The Type III, unimodal, relatively well sorted; (d) The Type IV, unimodal, well sorted; (e) The Type V, bimodal, poorly sorted; (f) The Type VI, unimodal, relatively well sorted.

## 5. Discussion

### 5.1. Effect of Sedimentation on Reservoir

#### 5.1.1. Microfacies and Facies

Fourteen microfacies were identified in the Yamama Formation based on indication biology, grain size, sorting, texture, and structure. The characteristics of each microfacies are summarized in Table 1. Based on the microfacies assemblages in the coring wells, six facies were identified, i.e., open shelf, patchy reef, shoal, back shoal, lagoon, and supratidal flat. The contact relationship of each facies is determined in the coring wells. Finally, a semi-restricted carbonate ramp model was established for the Yamama Formation in X Oilfield (Figure 10).

#### (1) Open shelf

The open shelf belongs to the middle-outer ramp, under the fair weather wave base (FWWB), which is open and deep with low hydrodynamics (Figure 10). It includes MF2, MF13, and MF14. The sediments have a high clay content. The core is light yellow, mostly dense, and patchy burrows can be seen. On the cast thin sections, mudstone, wackstone, and a few dolomites can be observed, and some burrows are mostly filled by calcite. The open shelf is mainly developed in the lower part of the YRC member and the lower part of the YRB member.

**Table 1.** Microfacies and characteristics of Yamama Formation in X oilfield.

Microfacies	Biology and Proportion %	Sorting	Size/ $\mu\text{m}$	Textxure	Other Bioclastic	Structure	Proportion/%
MFT1	Dolomite (>50) Gypsum (10~35)	Good	30~50	/	Residual bioclastic	Fine crystalline	2.7
MFT2	/	/	/	bioturbation	<i>Algae / Bivalve / Peloids, Benthic Foraminifera / Echinoderms / Gastropods</i>	W/P	6.8
MFT3	<i>Algae</i> (10~32)	Poor	50~1000	/	<i>Benthic Foraminifera and Bivalve, few corals / sponge / Echinoderms, Gastropods / Peloids</i>	W/P	22.0
MFT4	<i>Algae</i> (10~33) <i>Bivalve</i> (10~26)	Poor	<i>Algae</i> 50~1000 <i>Bivalve</i> 500~2000	/	<i>Benthic Foraminifera / Peloids / Echinoderms / sponge / corals</i>	W/P	10.9
MFT5	<i>Algae</i> (12~26) <i>Peloids</i> (10~40)	Poor Medium	<i>Algae</i> 200~1000 <i>Peloids</i> 100~500	/	<i>Benthic Foraminifera and Bivalve 6~30%, few Echinoderms / Rusdist / corals / sponge</i>	W/P	9.6
MFT6	<i>Bacinella</i> (10~25) <i>Algae</i> (10~35) <i>Peloids</i> (10~38)	Poor Poor Medium	<i>Bacinella</i> >2000 <i>Algae</i> >300 <i>Peloids</i> 100~500	/	<i>Benthic Foraminifera dominated, few Bivalve / Echinoderms</i>	B	9.4
MFT7	<i>Algae</i> (10~33) <i>Corals</i> (10~40)	Poor	<i>Algae</i> 100~1000 <i>Corals</i> >1000	/	<i>Peloids and Bivalve dominated, few Benthic Foraminifera / Echinoderms</i>	F	3.3
MFT8	<i>Corals and Sponge</i> (10~35)	Poor	<i>Corals and sponge</i> >2000	/	<i>Benthic Foraminifera / Peloids / Bivalve / Echinoderms</i>	F	3.9
MFT9	<i>Peloids</i> (10~60)	Medium	<i>Peloids</i> 100~300	/	<i>Benthic Foraminifera dominated, few Bivalve / Echinoderms / Algae</i>	W-P	5.3
MFT10	<i>Peloids</i> (10~55)	Medium	<i>Peloids</i> 100~500 Other bioclastic 200~800	/	<i>Benthic Foraminifera / Bivalve / Echinoderms dominated, few Algae / sponge</i>	P	8.6
MFT11	<i>Peloids</i> (15~60)	Good Poor	<i>Peloids</i> $\approx$ 300 Bioclastic 300~2000	/	<i>Benthic Foraminifera, Bivalve / Echinoderms dominated, few Algae</i>	G	5.1
MFT12	<i>Peloids</i> (25~65)	Good	<i>Peloids</i> $\approx$ 100 Bioclastic 200~300	/	<i>Echinoderms dominated, follwed by Benthic Foraminifera / Bivalve</i>	G	2.7

Table 1. Cont.

Microfacies	Biology and Proportion %	Sorting	Size/ $\mu\text{m}$	Textxure	Other Bioclastic	Structure	Proportion/%
MFT13	bioclastic (22~60)	Good	Bioclastic $\approx 50 \mu\text{m}$	/	Algae/Bivalve dominated, few sponge/Peloids	W	4.7
MFT14	Bioclastic (9~44)	Good	Bioclastic $<100 \mu\text{m}$	/	Benthic Foraminifera/Bivalve/Algae/Ostracods/Sponge spicule/Gastropods	M-W	4.8

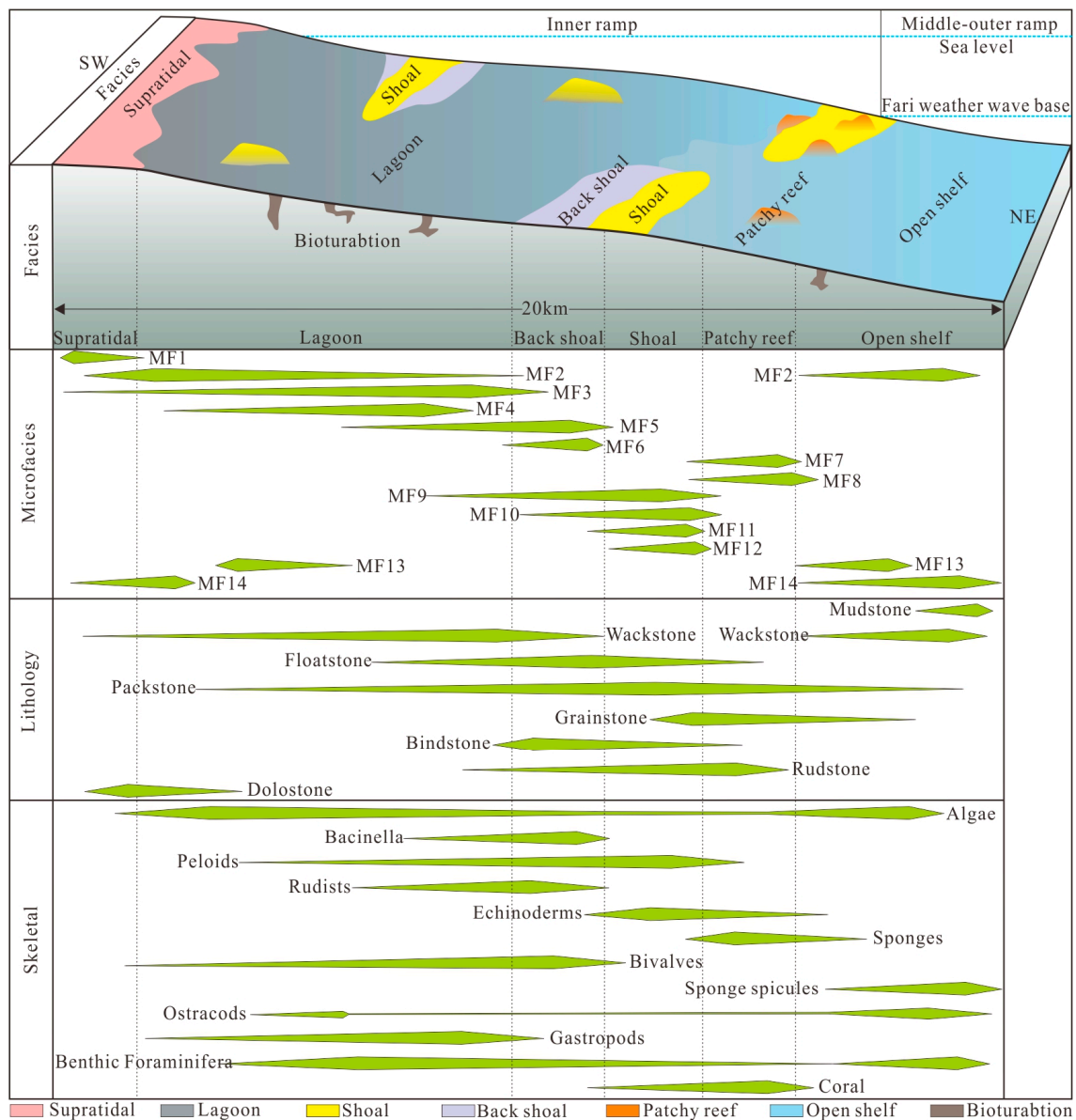


Figure 10. Depositional model of the Yamama Formation in X oilfield and effect on reservoir.

(2) Patchy reef

Patchy reef is near the FWWB with open shallow water, where the nutrients are sufficient and hydrodynamics are stronger (Figure 10). The patchy reef includes MF7 and MF8. The sediments are clean with little micrite. The core is dark gray, with white cement

visible between the grains. On the core, large fragments, such as corals and sponges, are visible. On the cast thin sections, corals and sponges are filled with calcite, which are relatively well preserved and easy to recognize. Patchy reef is mainly developed in YRC member or the lower of YRB member.

### (3) Shoal

Shoal is near the FWWB with the strongest hydrodynamics, belonging to inner ramp (Figure 10). The sediments are clean with little micrite, and the grains are well sorted. The shoal includes MF9, MF10, MF11, and MF12. The core is dark brown, and locally is gray due to the cementation. On the cast thin sections, peloids and *Echinoderms* are dominant, with a small number of *Benthic Foraminifera* and other bioclasts. The peloids are better sorted and rounded, and intergranular pores are developed. The shoals are mainly developed in the YRB member or the lower part of the YRC member.

### (4) Back shoal

Back shoal belongs to inner ramp, above the FWWB (Figure 10). The back shoal is deposited in relatively open water, where the nutrients are sufficient and the hydrodynamics are weaker. The back shoal includes MF5 and MF6 and is dominated by bindstone. The sediment has a high micrite content. The core is dark brown, with local cementation resulting in a dark gray color. On cast thin sections, large *Bacinella* and a large number of skeletal pores can be seen, or some pores are filled with calcite. Few *Algae* and peloids are distributed in the matrix. The back shoal is mainly developed in the YRA member.

### (5) Lagoon

Lagoon belongs to the inner ramp, above FWWB, where water is semi-restricted due to the partial block by patchy reefs, shoal, and back shoal (Figure 10). The lagoon is shallow, but the hydrodynamics are relatively low and the sediment has high micrite content. In lagoon, biology is flourishing and diversified, and the bioturbation is common. It includes MF2, MF3, MF4, MF5, MF13, and MF14. The core is dark brown, with grains invisible to the naked eye, and the local cementation causes the core to be light gray and dense. On cast thin sections, many *Algae*, moldic pores, or pores densely filled by cementation can be seen. *Gastropods*, *Benthic Foraminifera*, and peloids are also visible. The lagoon is widely developed in the YRB member and the YRA member.

### (6) Supratidal flat

Supratidal flat is above the mean high tide base and is only submerged during storms (Figure 10). Under arid climate conditions, penecontemporaneous dolomitization occurs, forming thin dolostone. The supratidal flat includes MF1, MF2, MF3, and MF14. The core is dark gray, and the local dolomitization becomes dark green. On the cores, different colors are interlayered, and the whole core is relatively dense. On the cast thin sections, *Algae* is discretely distributed in the micrite, and a large amount of fine dolomite and residual lime mud can be seen. The supratidal flat is mainly developed in YB-1 member and Yamama Upper member and locally developed in YRB member.

## 5.1.2. Depositional Model

Sedimentation had an important influence on the reservoir lithology, structure, and components [16,32,33]. As shown in Figure 10, the supratidal flat is dominated by dolomites. The lagoon is dominated by wackstone and packstone, with many kinds of bioclastic, mainly *Algae*, *Benthic Foraminifera*, *Ostracods*, and *Gastropods*, and contains a small number of peloids and *Bivalve*. Patchy reefs are dominated by floatstone and packstone, with bioclastic dominated by *Corals*, *Sponges*, and a few *Rudist*. The back shoal is dominated by bindstone accompanied by packstone and floatstone, and the bioclastic is dominated by *Bacinella* and peloids containing *Algae* and *Bivalves*. The shoal is dominated by grainstone, rudstone, and packstone, whose grains are dominated by peloids and *Echinoderms*. The open shelf is dominated by wackstone, locally containing mudstone, and the bioclastic is dominated by *Algae*, *Spicule Sponge*, and *Ostracods*.

### 5.1.3. Sediments and Pores Types

The sediments of the Yamama Formation are rich in bioclastic, and also contain peloids. Grain components have an important influence on pore types. Sediments rich in peloids are prone to develop intergranular pores. Dissolution of *Algae* can form moldic pores or vuggy pores. *Bacinella*, *Benthic Foraminifera*, and other aragonite or high magnesium bioclastic is easy to dissolve forming skeletal pores. Micropores are developed in micrite.

For example, at 3884.33 m, 3927.53 m, and 4071.52 m, when the peloids are better developed, the depth corresponding to them seems to have more intergranular pores (Figure 11). From 4025.76 m to 4036.8 m, the samples are rich in *Algae* and its moldic pore also developed. With the increase of *Algae* content, the volume of moldic pores increased (Figure 11). The skeletal pores are mainly controlled by the *Bacinella* and *Benthic Foraminifera*, and other bioclastic, such as *Corals* and *Sponges*, can also develop a small number of skeletal pores. For example, at 3927.53 m, the *Bacinella* are the most developed, and their corresponding depth skeletal pores are also the highest (Figure 11). From 3884.33 m to 3900.54 m and from 3977.77 m to 4018.31 m, the micrite is richer and its corresponding depth micropores are also better developed (Figure 11).

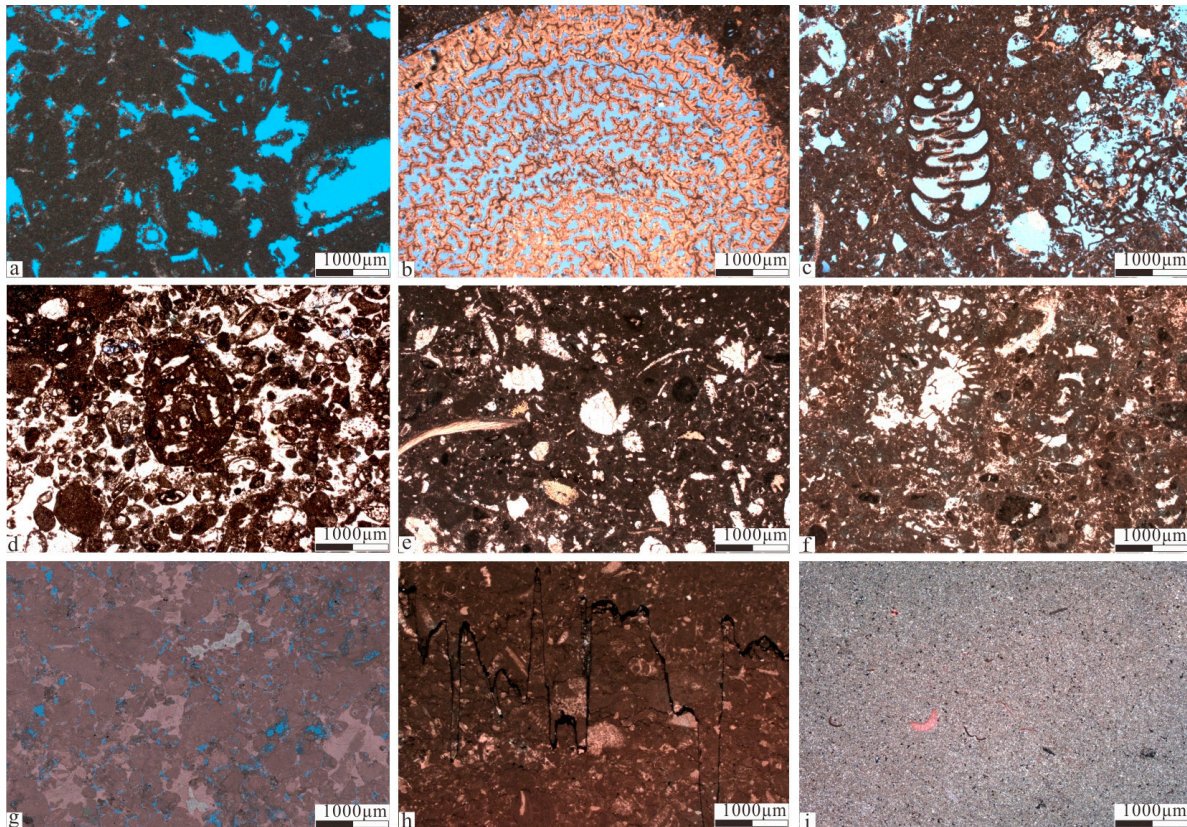


Figure 11. Effect of grains type and content on reservoir pore.

### 5.2. Effect of Diagenesis on Reservoir

Based on the 881 cast thin sections, the diagenesis of the Yamama Formation in the X oilfield includes dissolution, cementation, micritization, compaction, pressolution, and dolomitization. Dissolution is the most important constructive diagenesis, and it is the main reason for the formation of secondary pores, such as moldic pores and skeletal pores

(Figure 12a–c). The physical properties of all lithologies can be improved after dissolution. The physical properties are severely damaged by cementation, which can densely fill intergranular pores or moldic pores (Figure 12d,e). Micritization has a negative effect on the reservoir physical properties, and *Benthic Foraminiferal* usually undergone serious micritization, and the scattered micrite can fill the pores (Figure 12f). Compaction mainly affects the peloids, causing the peloids to flatten, reducing the pore volume, blocking the pore throat, and reducing the physical properties (Figure 12g). Pressolution and dolomitization are only locally developed, which have unfavorable effects on reservoir properties (Figure 12h,i).



**Figure 12.** Diagenesis of the Yamama Formation in the X oilfield. (a) W-005 well, dissolution; (b) W-001 well, dissolution; (c) W-001 well, dissolution; (d) W-001 well, cementation; (e) W-001 well, cementation; (f) W-001 well, micritization; (g) W-006 well, compaction; (h) W-002 well, pressolution; (i) W-003 well, dolomitization.

Diagenesis could lead to physical differentiation of the same microfacies. Dissolution and cementation have the most significant effects on the physical properties. As shown in Figure 13, after intense dissolution of peloids grainstone, *Algae* wackstone, and *Bacinella* bindstone, a large number of intergranular dissolution pores, moldic pores, and skeletal pores can be seen in the cast thin sections, with the porosity greater than 20% and the permeability greater than 10 mD (Figure 13a–c). However, if the same microfacies undergo intense cementation, the pores will be densely filled with cement, the pores cannot be seen on casting thin section by naked eyes, the porosity is usually less than 10%, and the permeability is less than 1 mD (Figure 13d–f).

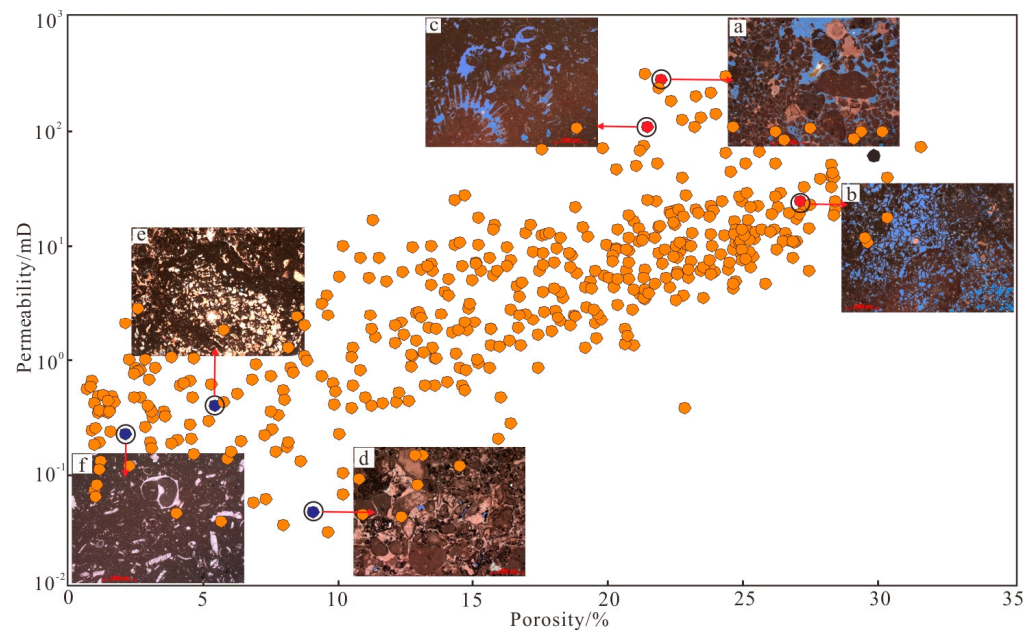


**Figure 13.** Effect of diagenesis on reservoir physical properties of the Yamama Formation. (a) peloids grainstone, intense dissolution; (b) *Bacinella* bindstone, intense dissolution; (c) *Algae* wackstone, intense dissolution; (d) peloids grainstone, intense cementation; (e) *Bacinella* bindstone, intense cementation; (f) *Algae* wackstone, intense dissolution, intense cementation.

### 5.3. Effect of Sequence on Reservoir

Based on core and cast thin section data, three types of key sequence boundary were identified in the Yamama Formation of the X Oilfield.

The first type of sequence boundary is the facies mutation surface, which is two different sedimentary facies above and below the boundary. The water depth, hydrodynamics, structure, and components of the two facies are significantly different. Normally, above the boundary is a deep-water environment with weak hydrodynamics (Figure 14a), while below the boundary is a shallow water environment with strong hydrodynamics (Figure 14b). The boundary between the two facies is clear and is easy to be recognize, which indicates abrupt rise of sea level. This boundary is developed at the top of the YRC member. Below the boundary is a patchy reef or shoal grainstone and rudstone, with a core thickness of nearly 10 m, and on cast thin sections, well-sorted peloids and large bioclasts with strong cementation are shown. Above the boundary is open shelf mudstone and wackstone, with a dense and bioturbated core. The boundary is easy to recognize by its lithology, color, and structure.

The second type is the boundary of evaporite changing to limestone; this type of boundary is essentially a facies mutation surface. Below the boundary is the supratidal flat mudstones or dolomites, with gypsum locally visible, and above the boundary is the lagoon or open shelf wackstone or mudstone. This sequence boundary reflects a drop of sea level to a minimum and the formation exposure to an arid environment, followed by a slow or sudden rise in sea level and a return to normal carbonate deposition. This kind of sequence boundary is developed at the top of the Yamama Upper member and YB-2 member. Below the boundary are thin dolomite and thick mudstone interbedded, with light gray dense cores; fine dolomite and gypsum can be seen on cast thin sections (Figure 14c). Above the boundary is lagoons or open shelf. The boundary is similar in color and structure and is not easily recognized.

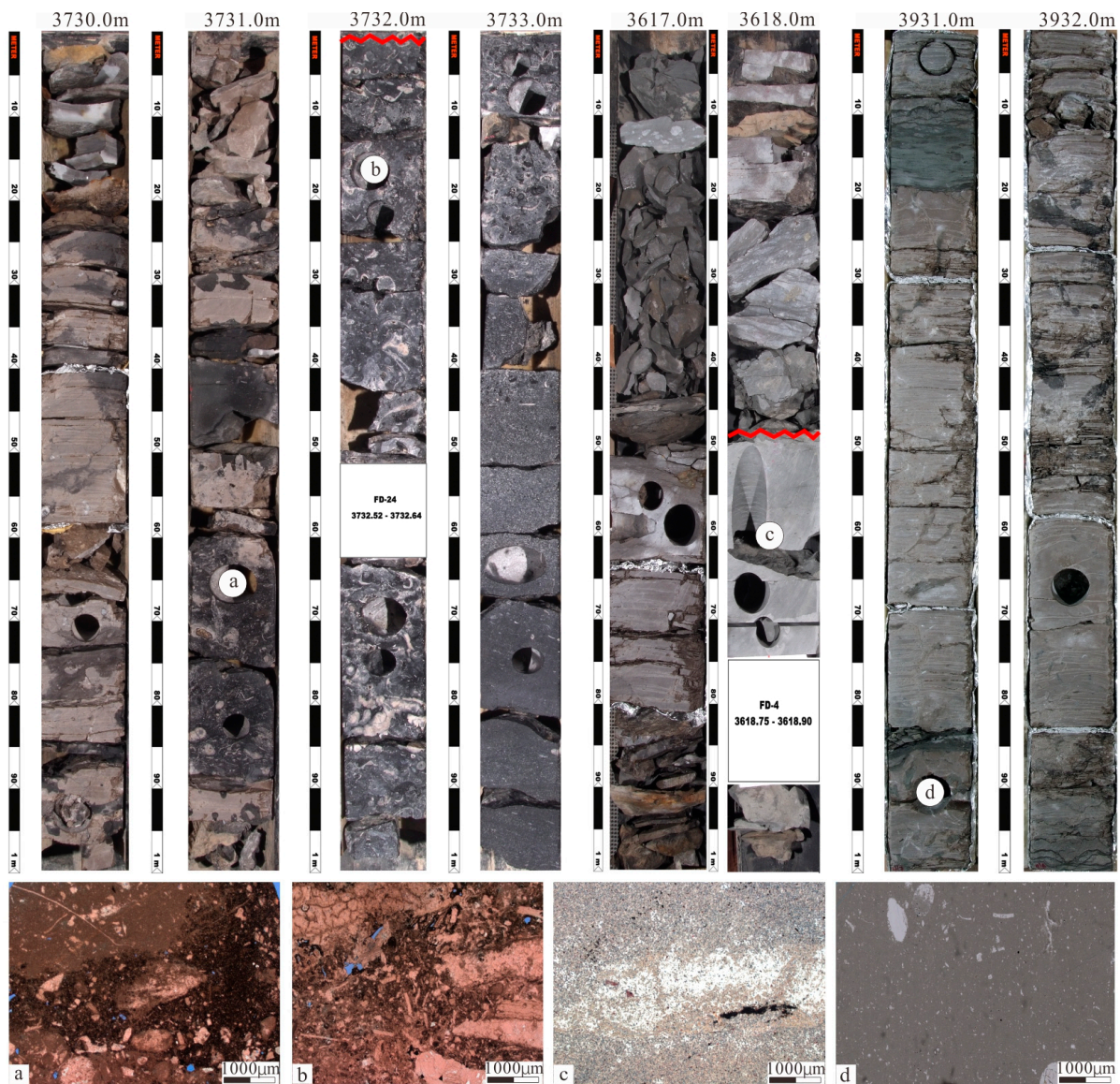


**Figure 14.** Key sequence boundary of the Yamama Formation in X oilfield (the red wavy lines are the sequence boundary). (a) W-002 well; (b) W-002 well; (c) W-006 well; (d) W-006 well.

The third boundary is the maximum flooding surface (MFS). Since the Yamama Formation was mainly deposited in shallow water, the condensed section is not developed, even during the MFS. In general, the time when the grains content changes from high to low and then to high can be identified as the MFS. There is biology present indicative of deep-water conditions, such as *Planktonic foraminifera* and *Sponge spicule*; it can also be identified as the MFS. The MFS of the Yamama Formation on the core is light gray and dense, and locally dark green and bioturbated. On cast thin sections, wackstone with unsorted bioclastic such as *Algae*, *Gastropods*, and *Benthic Foraminifera* can be seen. MFS are developed at the top of YB-2 member, the top of YB-1 member, and the upper of Yamama member. It should be noted that the sea level of the Yamama Formation is decreasing, and the MFS is less distinctive from the bottom to the top.

Three sequences were identified in the Yamama Formation, namely sequence I (YRC and YB-2), sequence II (YRB and YB-1), and sequence III (YRA and Yamama Upper) (Figure 15).

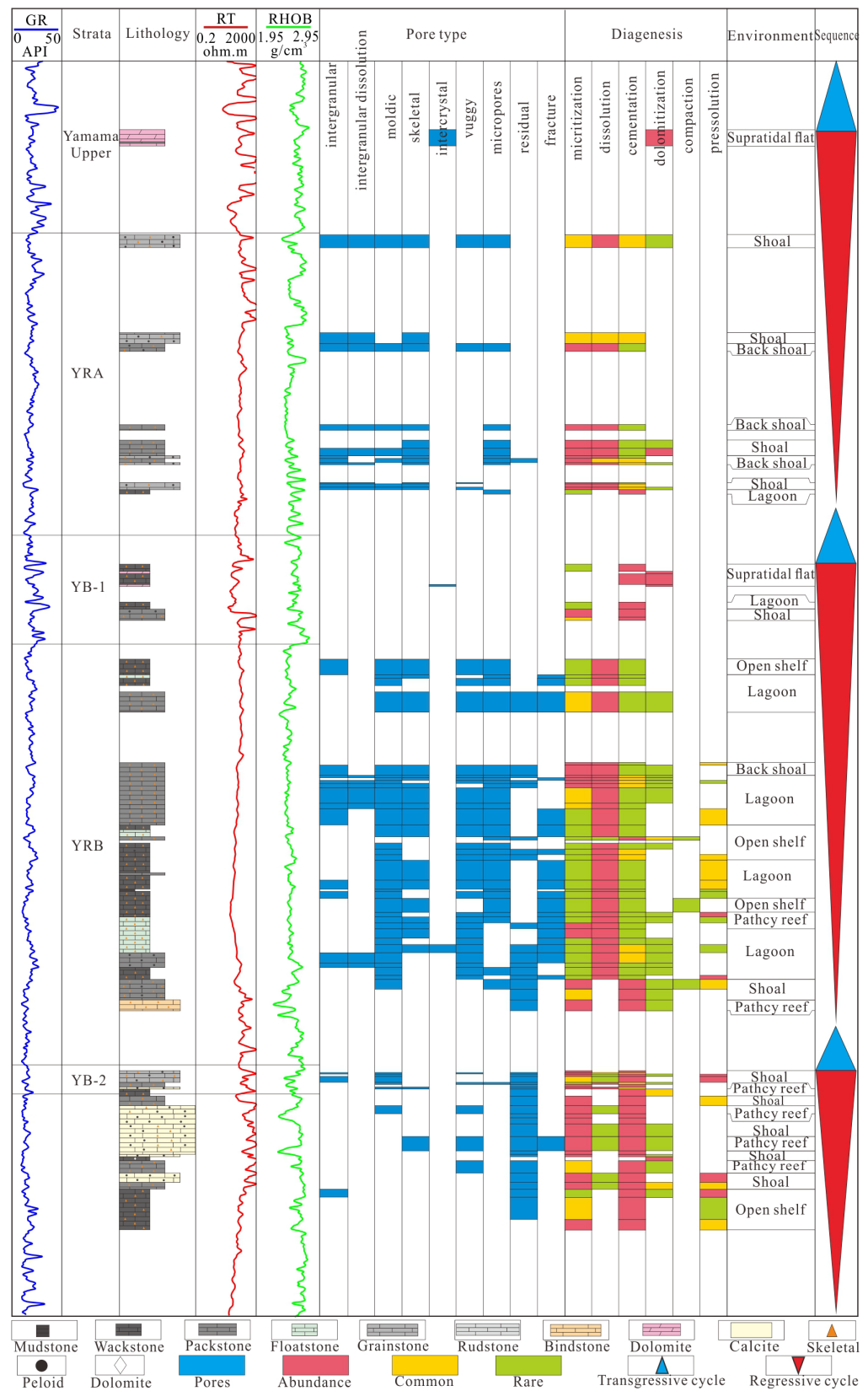


Figure 15. Effect of sequence on reservoirs quality and heterogeneity.

5.3.1. Sequence I

This is the lowermost sequence interpreted in the Yamama Formation within the study area. The regressive cycle began with an open shelf and gradually evolved into patchy reefs

and shoal. The lithology is interbedded with grainstone and packstone. Dissolution and cementation coexist, but cementation dominates. The pores are characterized by residual pores. To the late regressive cycle, it evolves into a lagoon, accompanied by small scale patchy reefs, and the lithology is dominated by wackstone, with intense micritization and cementation (Figure 15).

### 5.3.2. Sequence II

The depositional environment changed drastically from patchy reef or shoal to lagoon or open shelf. The transgressive cycle is dominated by wackstone, mudstone, or dolostone until the MFS, where the cementation is common and the reservoir is tight. The regressive cycle began with open shelf, and then lagoon and patchy reef frequently evolved alternately, with intense dissolution and light cementation, and the pores were mainly moldic pores, micropores, and residual pores, with a low degree of development of intergranular pores. At the late regressive cycle, shoal and supratidal flat are developed, cementation and dolomitization are intense, and the reservoir is tight (Figure 15).

### 5.3.3. Sequence III

With the rapid rise of the sea level, the open shelf overlies the supratidal flat until the MFS. The transgressive cycle is characterized by intense cementation and the reservoir is tight. The regressive cycle began with open shelf, and then lagoon, shoal, and back shoal evolved frequently and alternately, with intense micritization, dissolution, and local cementation in shoal. The pores include intergranular pores, moldic pores, skeletal pores, micropores, and residual pores. In the middle stage of the regressive cycle, the lagoon, back shoal, and shoal evolve alternately. Dissolution and cementation coexist, but dissolution dominates. The pores are dominated by moldic pores and residual pores. In the late stage of the regressive cycle, supratidal flat deposits are dominated, with strong cementation and dolomitization, and the reservoir is tight. In the transgressive cycle, the open shelf covers the supratidal flat again (Figure 15).

## 5.4. Distribution of Favorable Reservoir

Overall, the sedimentary facies change frequently with the sequences, and the same sedimentary facies undergoes different types and intensities of diagenesis during sea level cycle changes, resulting in prominent differences in pore types and physical properties [34].

Diagenesis controls reservoir development extent and reservoir quality in each member. In the YRC member, although it was characterized by high and open depositional facies, the diagenesis is dominated by cementation; therefore, the reservoir in YRC is less developed or the reservoir has poor quality. However, for the YRA member and YRB member, the diagenesis is dominated by dissolution. Therefore, the reservoir in these two members is highly developed and the physical property is relatively better.

In the YRA member and YRB member, the sedimentation had an important influence on the reservoir quality. The high energy facies, such as shoal, back shoal, and patchy reef, in combination with dissolution could form favorable reservoirs. The lagoon, rich in *Algae* that has undergone intense dissolution, could also form a favorable reservoir. Favorable reservoir refers to a reservoir whose porosity is greater than 10% and permeability greater than 1 mD.

Based on the sedimentation in the YRA member and YRB member, in combination with seismic inversion, the distribution of favorable reservoirs is delineated. In the YRA member, the favorable reservoir is mainly distributed on the north-central part of study area, with a small amount in the axis of the southern part of the study area (Figure 16a). In the YRB member, the favorable reservoir is widely distributed. The favorable reservoir is mainly distributed in the north-central part of study area and is locally undeveloped. In the southern part of the study area, the favorable reservoirs are mainly distributed in the two flanks of the anticline (Figure 16b).

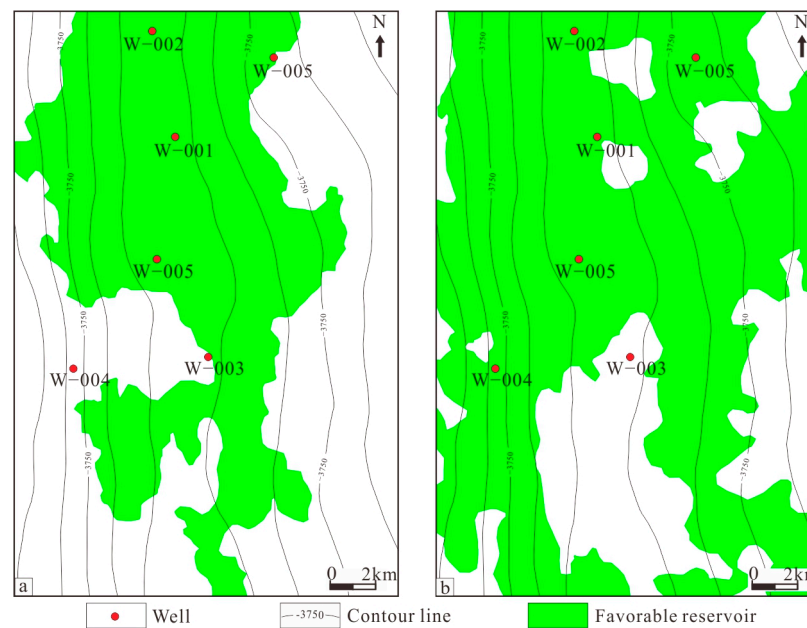


**Figure 16.** Distribution of Favorable Reservoir of the Yamama Formation in X Oilfield. (a) Distribution of Favorable Reservoir of YRA; (b) Distribution of Favorable Reservoir of YRB.

## 6. Conclusions

Eight lithologies are developed in the Yamama Formation, of which packstone and wackstone are dominant. The reservoirs are predominantly medium- to high-porosity, extra-low permeability, and tight. Nine types of pores are developed, of which moldic pores, micropores, and skeletal pores are the most developed. The reservoir of the Yamama Formation, therefore, is poor quality and is extremely heterogenous.

A carbonate ramp model was established, where the hydrodynamics were relatively weak, and the Yamama Formation was mainly deposited in a lagoon. The development potential for large-scale, high-quality reservoirs is low in such a semi-restricted depositional setting. High-energy sedimentary facies such as shoal, back shoal, and patchy reefs coupled with dissolution could form high-quality reservoirs. A lagoon rich in *Algae* that has undergone intense dissolution could form a medium-high porosity and low permeability reservoir. The favorable reservoir is mainly distributed in the YRA member and YRB member.

Diagenesis controls reservoir development extent and reservoir quality in different members. Sedimentation had an important influence on the reservoir quality. When the sea level cycles, the depositional environment evolves, and the diagenesis types and extent change continuously, which leads to difference of reservoir development in each member and differentiation of physical planes in the same member.

The eastern and southern parts of the study area were poorly served by wells and had high uncertainty in reservoir prediction. It is recommended that two appraisal wells be deployed in the eastern and southern flanks of the study area to implement reservoir quality and favorable reservoir development degree and distribution. Favorable reservoirs in the YRA and YRB are the most preferred targets for developing the Yamama formation.

**Author Contributions:** Conceptualization, Y.W. and F.L.; methodology, Y.W.; software, L.L.; validation, Y.W., F.L. and L.L.; formal analysis, H.C.; investigation, L.L.; resources, H.C.; data curation, W.W.; writing—original draft preparation, Y.W.; writing—review and editing, F.L.; visualization, H.C.; supervision, W.W.; project administration, W.W.; funding acquisition, W.W. All authors have read and agreed to the published version of the manuscript.

**Funding:** This research was funded by CNPC prospective and fundamental project: “The Theory and Key Technology Research on Efficient Development of Abnormal High-Pressure, Sour, Light

Oil Carbonate Reservoirs” (grant number 2022DJ3211) and CNPC key scientific and technological projects “Research and application of key technologies for water injection development in thick carbonate reservoir” (grant number 2023ZZ19-01).

**Institutional Review Board Statement:** Not applicable.

**Informed Consent Statement:** Not applicable.

**Data Availability Statement:** No new data were created or analyzed in this study. Data sharing is not applicable to this article.

**Acknowledgments:** Jiquan Yin, and Zhaohui Xia from RIPED are thanked for their insightful discussions. PETROCHINA is thanked for access to the data and permission to publish.

**Conflicts of Interest:** Authors Fengfeng Li, Lei Li, Haowei Chen, Wenyu Wang and Yang Wan was employed by the company Research Institute of Petroleum Exploration and Development, Petrochina. The authors declare that the research was conducted in the absence of any commercial or financial relationships that could be construed as a potential conflict of interest.

## References

- Steinke, A.; Bramkamp, R.A. Mesozoic rocks of eastern Saudi Arabia (abs.). *AAPG Bull.* **1952**, *36*, 909.
- Al-Siddiki, A.A.M. Subsurface geology of southeastern Iraq. In Proceedings of the 10th Arab Petroleum Congress, Tripoly, Libia, 16–22 January 1978; p. 141.
- Handhal, A.M.; Al-Najm, F.M.; Chafeet, H.A. Determination of flow units of Yamama Formation in the West Qurna oil field, Southern Iraq. *Iraqi J. Sci.* **2018**, *59*, 1878–1898.
- Idan, R.M.; Salih, A.L.; Al-Khazraji, O.N.; Khudhair, M.H. Depositional environments, facies distribution, and porosity analysis of Yamama Formation in majnoon oilfield. Sequence stratigraphic approach. *Iraqi Geol. J.* **2020**, *53*, 38–52. [[CrossRef](#)]
- Jassim, S.Z.; Buday, T. Late Tithonian—Early Turonian Megasequence AP8. In *Geology of Iraq*; Jassim, S.Z., Goff, J.C., Eds.; Dolin, Prague and Moravian Museum: Brno, Czech Republic, 2006; Chapter 11; pp. 156–183.
- Sadooni, F.N. Stratigraphic sequence, microfacies, and petroleum prospects of the Yamama Formation, Lower Cretaceous, Southern Iraq. *AAPG Bull.* **1993**, *77*, 1971–1988.
- Douban, A.F.; Medhadi, P. Sequence chronostratigraphy and petroleum systems of the Cretaceous Megasequences, Kuwait. *AAPG Int. Conf. Exhib.* **1999**, 152–155.
- Alsharhan, A.S.; Nairn, A.E.M. A review of the Cretaceous formations in the Arabian Peninsula and Gulf: Part I. Lower Cretaceous (Thamama Group) stratigraphy and paleogeography. *J. Pet. Geol.* **1986**, *9*, 365–391. [[CrossRef](#)]
- Alsharhan, A.S.; Nairn, A.E.M. A review of the cretaceous formation in the Arabian Peninsula and Gulf: Part II. Mid-Cretaceous (Wasia Group) stratigraphy and paleogeography. *J. Pet. Geol.* **1988**, *11*, 89–112. [[CrossRef](#)]
- Alsharhan, A.S.; Nairn, A.E.M. A review of the Cretaceous formations in the Arabian Peninsula and Gulf: Part III. Upper Cretaceous (Aruma Group) stratigraphy and paleogeography. *J. Pet. Geol.* **1990**, *13*, 247–266. [[CrossRef](#)]
- Al-Ibrahim, R.N.; Al-Ameri, T.K. Crude oil analyses of the Yamama Formation in the Subbah, Ratawi, Tuba and Luhis oil fields, Southern Iraq. *Iraqi J. Sci.* **2015**, *56*, 1425–1437.
- Al-Marsoumi, A.M.H.; Abdul-Wahab, D.S. Hydrogeochemistry of Yamama Reservoir formation water-west Qurna oil field-Southern Iraq. *Basrah J. Sci.* **2005**, *23*, 10–20.
- Al-Khafaji, A.J.; Al Najm, F.M.; Al Ibrahim, R.N.; Sadooni, F.N. Geochemical investigation of Yamama crude oils and their inferred source rocks in the Mesopotamian Basin, Southern Iraq. *Pet. Sci. Technol.* **2019**, *37*, 2025–2033. [[CrossRef](#)]
- Al-Khafaji, A.J.; Al-Najm, F.M.; Al-Refai, R.A.; Sadooni, F.N.; Al-Owaidi, M.R.; Al-Sultan, H.A. Source rock evaluation and petroleum generation of the Lower Cretaceous Yamama Formation: Its ability to contribute to generating and expelling petroleum to cretaceous reservoirs of the Mesopotamian Basin, Iraq. *J. Pet. Sci. Eng.* **2022**, *217*, 110919. [[CrossRef](#)]
- Saleh, A.H. Microfacies and environmental study of the lower cretaceous yamama formation in Ratawi field. *Arab. J. Geosci.* **2014**, *7*, 3175–3190. [[CrossRef](#)]
- Mohsin, S.A.; Mohammed, A.H.; Alnajm, F.M. Microfossils (Foraminifera and Calcareous Algae) of the Yamama Formation, Southern Iraq. *Iraqi Geol. J.* **2022**, *55*, 109–126. [[CrossRef](#)]
- Al Mafraji, T.G.Z.; Al-Zaidy, A.A.H. Microfacies architecture and stratigraphic development of the Yamama Formation, southern Iraq. *Iraqi J. Sci.* **2019**, *60*, 1115–1128. [[CrossRef](#)]
- Ahmed, M.A.; Nasser, M.E.; Jawad, S.N.A.L. Diagenesis processes impact on reservoir quality in carbonate Yamama Formation/Faiha Oil Field. *Iraqi J. Sci.* **2020**, *61*, 92–102. [[CrossRef](#)]
- Handhal, A.M.; Chafeet, H.A.; Dahham, N.A. Microfacies, depositional environments and diagenetic processes of the Mishrif and Yamama formations at Faiha and Sindibad oilfields, south Iraq. *Iraqi Bull. Geol. Min.* **2020**, *16*, 51–74.
- Al-Baldawi, B.A. Evaluation of petrophysical properties using well logs of yamama Formation in abu amood oil field, southern Iraq. *Iraqi Geol. J.* **2021**, *54*, 67–77. [[CrossRef](#)]
- Chafeet, H.A. Yamama reservoir characterization in the West Qurna oil field, Southern Iraq. *Iraqi J. Sci.* **2016**, *57*, 938–947.

22. Nasser, M.E.; Al-Jawed, S.N.; Hassan, M.F. Geological modeling for Yamama Formation in Abu Amood oil field. *Iraqi J. Sci.* **2017**, *58*, 1051–1068.
23. Al-Khafaji, A.J. The Mishrif, Yamama, and Nahr Umr reservoirs petroleum system analysis, Nasiriya oilfield, Southern Iraq. *Arab. J. Geosci.* **2015**, *8*, 781–798. [[CrossRef](#)]
24. Al-Obaidi, M.; Ahmed, M.T.; Khwedim, K.; Hussain, S.A. Paleoredox and Environmental Conditions of Southern Neo-Tethys Deposits in South Iraq (Yamama Formation) by Geochemical Indicators. *Iraqi J. Sci.* **2020**, *61*, 2619–2627. [[CrossRef](#)]
25. Dunnington, H.V. Generation, migration, accumulation, and dissipation of oil in northern Iraq. In *Habitat of Oil*; Weeks, L.G., Ed.; AAPG: Tulsa, OK, USA, 1958; pp. 1194–1251.
26. Aqrabi, A.A.M.; Goff, J.C.; Horbury, A.D.; Sadooni, F.N. *The Petroleum Geology of Iraq*; Scientific Press: Beaconsfield, UK, 2010.
27. Ziegler, M.A. Late Permian to Holocene paleofacies evolution of the Arabian Plate and its hydrocarbon occurrences. *GeoArabia* **2001**, *6*, 445–504.
28. Haq, B.U.; Hardenbol, J.; Vail, P.R. Mesozoic and Cenozoic chronostratigraphy and cycles of sea-level change. In *Sea-Level Changes: An Integrated Approach*; Wilgus, C.K., Hastings, B.S., Kendall, C.G.S.C., Posamentier, H., Van Wagoner, J., Ross, C.A., Eds.; Society of Economic Paleontologists and Mineralogists, Special Publication; SEPM (Society for Sedimentary Geology): Claremore, OK, USA, 1988; Volume 42, pp. 71–108.
29. Dunham, R.J. *Classification of Carbonate Rocks According to Depositional Textures*; AAPG: Tulsa, OK, USA, 1962; Volume 38, pp. 108–121.
30. Flügel, E.; Munnecke, A. *Microfacies of Carbonate Rocks: Analysis, Interpretation and Application*; Springer: Berlin/Heidelberg, Germany, 2010.
31. Ministry of Energy, the People's Republic of China. *Oil Industry Standard Issued by the Ministry of Energy, the People's Republic of China: Evaluating Methods of Oil and Gas Reservoirs: SY/T 6285—2011[S]*; Ministry of Energy, the People's Republic of China: Beijing, China, 2011; p. 2.
32. Mahdi, T.A.; Aqrabi, A.A.M.; Horbury, A.D.; Sherwani, G.H. Sedimentological characterization of the mid-Cretaceous Mishrif reservoir in southern Mesopotamian Basin, Iraq. *GeoArabia* **2013**, *18*, 139–174. [[CrossRef](#)]
33. Mahdi, T.A.; Aqrabi, A.A.M. Role of facies diversity and cyclicity on the reservoir quality of the mid-Cretaceous Mishrif Formation in the southern Mesopotamian Basin, Iraq. *Geol. Soc. Lond. Spec. Publ.* **2017**, *435*, 1–21. [[CrossRef](#)]
34. Bromhead, A.D.; Van Buchem, F.S.P.; Simmons, M.D.; Davies, R.B. Sequence stratigraphy, palaeogeography and petroleum plays of the Cenomanian–Turonian succession of the Arabian plate: An updated synthesis. *J. Pet. Geol.* **2022**, *45*, 119–161. [[CrossRef](#)]

**Disclaimer/Publisher's Note:** The statements, opinions and data contained in all publications are solely those of the individual author(s) and contributor(s) and not of MDPI and/or the editor(s). MDPI and/or the editor(s) disclaim responsibility for any injury to people or property resulting from any ideas, methods, instructions or products referred to in the content.